

# Toward Oxidation-Resistant ZrB<sub>2</sub>-SiC Ultra High Temperature Ceramics

EMILY EAKINS, DONI DANIEL JAYASEELAN, and WILLIAM EDWARD LEE

Ultra high temperature ceramics (UHTCs), including ZrB<sub>2</sub>-SiC, are designed for extreme environment applications in which temperatures exceed 2273 K (2000 °C). A key material property of UHTCs in many applications is their resistance to oxidation. Recent research into UHTCs is described, revealing a variety of different methods for improving the oxidation performance, which include control of starting powders, composition and size distribution, mixing, and densification techniques. The use of additives has also been researched widely, for example, to increase the viscosity of any liquid phase formed or provide protective refractory phases at high temperatures. SiC additions are effective in forming protective silica but only in static environments and to ~1873 K (1600 °C). For higher temperature applications, additions of La lead to the formation of a dense ZrO<sub>2</sub> scale probably *via* liquid phase sintering. Such ceramic systems, which produce self-generating refractory oxidation barriers or dense ZrO<sub>2</sub> scales, show the greatest promise in providing oxidation-resistant UHTCs.

DOI: 10.1007/s11661-010-0540-8

© The Minerals, Metals & Materials Society and ASM International 2010

## I. INTRODUCTION

ULTRA high temperature ceramics (UHTCs) are designed to operate in extreme environments such as those experienced on leading edges of hypersonic vehicles or in propulsion components of missiles. In recent years, there has been a resurgence of interest in UHTCs, particularly methods of improving their high-temperature capabilities.

For UHTCs to maintain their structural integrity during service, exceptional oxidation resistance is paramount. Diborides of the transition metals such as hafnium and zirconium have proven to be some of the best candidate UHTC materials to date. For this review, only zirconium diboride-based ceramics will be considered unless research into hafnium diboride provides useful insight. Several reviews have summarized the history of UHTC research, material properties, and testing methods,<sup>[1,2]</sup> and these reviews consider the candidate materials and selection procedures necessary to produce a UHTC that fulfils the stringent requirements for these extreme environment applications.<sup>[3-5]</sup> The purpose of this review is to summarize the advances in research conducted in recent years that identify the possible methods of improving the oxidation resistance of existing UHTC materials.

## II. OXIDATION RESISTANCE AND METHODS FOR IMPROVEMENT

### A. Oxidation

The oxidation performance of zirconium diboride has been investigated since the 1960s,<sup>[6,7]</sup> and the temperature range in which the ceramics have been tested has increased with the testing capabilities of the time. For monolithic ZrB<sub>2</sub>, the oxide formed on oxidation is B<sub>2</sub>O<sub>3</sub>, which is liquid above 723 K (450 °C) and wets the oxide grains until it volatilizes at temperatures above 1373 K (1100 °C). Below 1373 K (1100 °C), the oxidation kinetics are controlled by the diffusion of oxygen through the liquid boron that surrounds the ZrO<sub>2</sub> grains. Between 1373 K and 1473 K (1100 °C and 1400 °C), the oxidation kinetics display parabolic characteristics because of the mass gain from ZrO<sub>2</sub> and B<sub>2</sub>O<sub>3</sub> formation, and mass loss from B<sub>2</sub>O<sub>3</sub> vaporization.

It has long been known that the addition of SiC improves the properties of ZrB<sub>2</sub> UHTCs significantly,<sup>[4,8-12]</sup> and it is concluded generally that the optimum amount of SiC is between 15 and 20 vol pct. The addition of SiC increases the sinterability of the starting powders by facilitating liquid phase sintering *via* formation of a borosilicate liquid. This in turn allows greater control of the diboride grain growth which has a beneficial effect on mechanical properties.<sup>[13,14]</sup> Other benefits reported include improved thermal shock resistance and oxidation resistance.<sup>[15]</sup> The impact of the presence of a connected low thermal conductivity and brittle glassy phase on thermal shock is likely to be limited since it will soften below 1273 K (1000 °C). During oxidation at elevated temperatures, the silicon from the SiC and boron from the ZrB<sub>2</sub> are oxidized to

---

EMILY EAKINS, PhD Student, DONI DANIEL JAYASEELAN, Post Doctoral Research Associate and WILLIAM EDWARD LEE, Professor, are with the Centre for Advanced Structural Ceramics (CASC) and Department of Materials, Imperial College, London SW7 2AZ, U.K. Contact e-mail: w.e.lee@imperial.ac.uk

Manuscript submitted June 7, 2010.

Article published online November 23, 2010

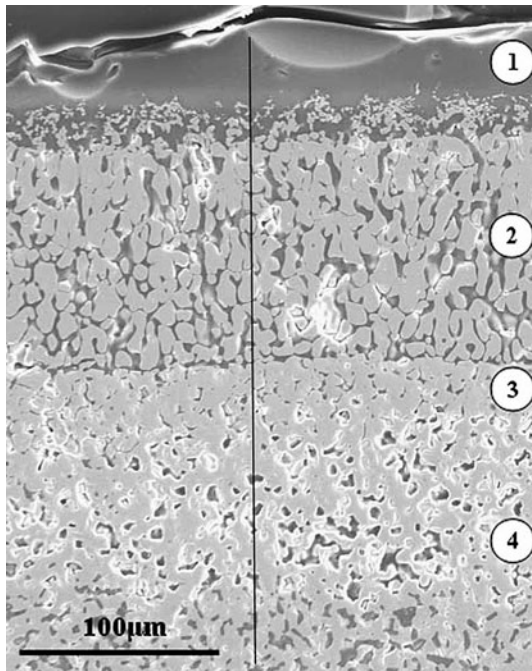
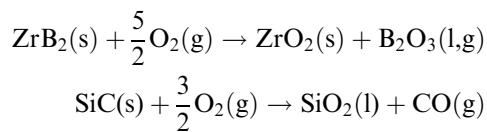


Fig. 1—Scanning electron microscope (SEM) image of  $\text{ZrB}_2 + 20$  vol pct SiC, after oxidation in air at 1900 K (1627 °C) for ten 10-min cycles. The numbers on the micrograph indicate: (1) outer glass layer, (2)  $\text{ZrO}_2$ -based interlayer, (3) SiC depleted zone, and (4) unreacted bulk ceramic.<sup>[10]</sup>

form a protective borosilicate glass layer according to the following equations:



Several researchers<sup>[10,16–18]</sup> found that the oxide scale generally has a layered structure (Figure 1 and Figure 2). A borosilicate glass layer is present at the top of the micrograph. Below this lies an oxide layer whose pores have become filled with a glassy phase. The high wetting angle between the oxide grain and borosilicate glass ensures complete protective coverage of the exposed faces below the temperature at which the glass evaporates. In some samples, there is a region below this oxide layer that is depleted in SiC. Finally, at the bottom of the micrographs is the unreacted bulk ceramic.

The borosilicate glass has a higher viscosity, higher boiling point, and lower vapor pressure than boria, providing more efficient oxidation protection. The effectiveness of the protective layer increases up to approximately 20 vol pct SiC. When  $\text{ZrB}_2$ -SiC materials undergo furnace oxidation at 1773 K (1500 °C), the thickness of the borosilicate layer decreases with increasing SiC content. When sufficient SiC is present, the borosilicate liquid flows from the site of oxidation toward the surface of the material and as the amount of SiC increases, the liquid can fill the spaces between the oxide grains efficiently to protect the material from subsequent oxidation.

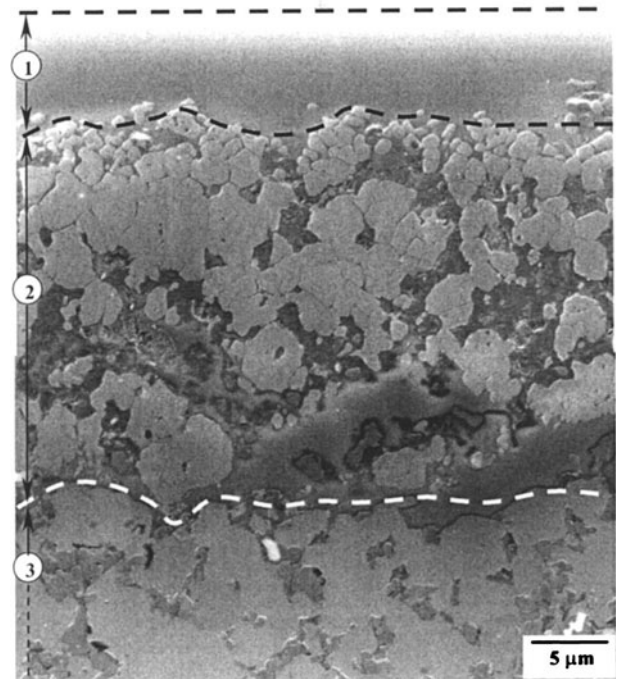


Fig. 2—SEM micrograph of the oxide scale in a  $\text{ZrB}_2 + 20$  vol pct SiC + 5 vol pct  $\text{Si}_3\text{N}_4$ , after nonisothermal oxidation testing up to 1623 K (1350 °C). The numbers on the micrograph indicate: (1) outer glass layer, (2)  $\text{ZrO}_2$ -based interlayer, and (3) unreacted bulk.<sup>[16]</sup>

The formation and efficacy of the oxidation microstructure has undergone extensive investigation. Li *et al.*<sup>[19]</sup> provided a detailed explanation of the mechanisms responsible for  $\text{ZrB}_2$ -SiC UHTCs improved oxidation performance over both monolithic  $\text{ZrB}_2$  and SiC. They suggested that the improved oxidation performance is caused by the development of a “solid pillars liquid roof” structure in which the borosilicate glass acts as a diffusion barrier and the  $\text{ZrO}_2$  grains retain the liquid and provide mechanical stability to the oxide layer. The oriented growth of the  $\text{ZrO}_2$  grains on oxidation of  $\text{ZrB}_2$ -SiC ceramics is caused by the production of gaseous by-products and direction of liquid transport.<sup>[20]</sup> The removal of  $\text{ZrO}_2$  grains occurs by the discharge of SiC gaseous products with high vapor pressures: carbon monoxide gas during passive oxidation and carbon monoxide and silicon monoxide gases during active oxidation.  $\text{ZrO}_2$  can be transported to the surface of the glass layer by convection or by reactions between the zirconia and the boria or silica.<sup>[20]</sup> Tailoring the glass composition to inhibit oxygen transport could slow down the progression of the oxide layer into the underlying bulk.

It is believed that the borosilicate liquid moves from the site of oxidation to the surface. This is thought to be caused by the silica liquids being nonwetting for zirconia and by the liquid phase being more viscous nearer the surface because of  $\text{B}_2\text{O}_3$  volatilization. Karlsdottir and Halloran<sup>[21]</sup> proposed that continued recession of the oxidation subscale during oxidation is caused by the flow of boria-rich liquid in “convection cells” between the oxide grains that provide transport paths for oxygen to progress into the, as yet unoxidized, bulk material.

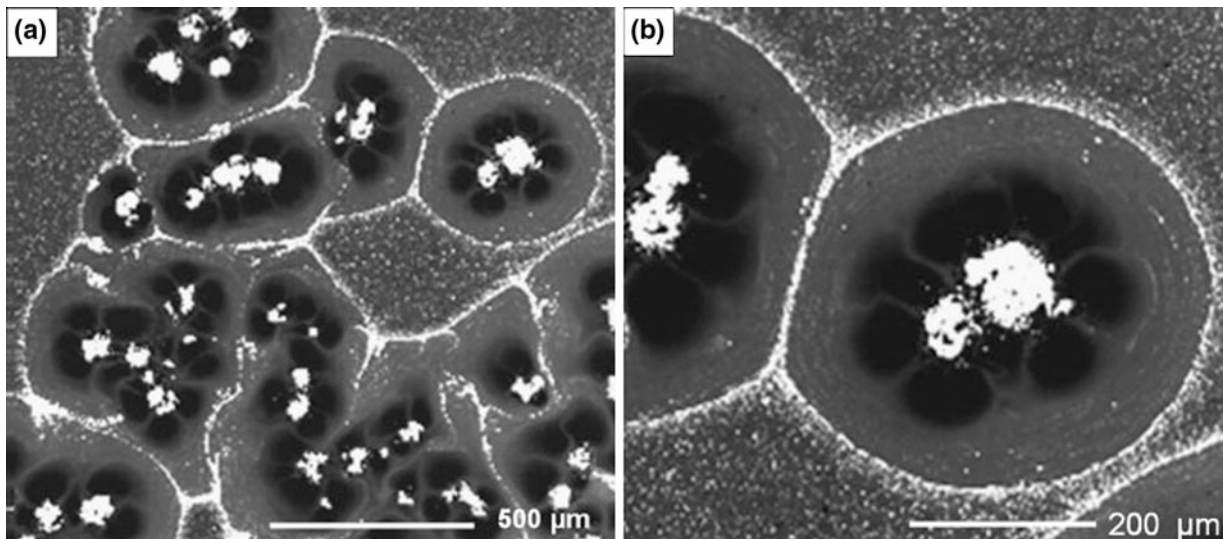


Fig. 3—Backscattered electron SEM images of convection cells on the surface of  $ZrB_2 + 15$  vol pct SiC after oxidation for 30 min at 1873 K (1600 °C).<sup>[21]</sup>

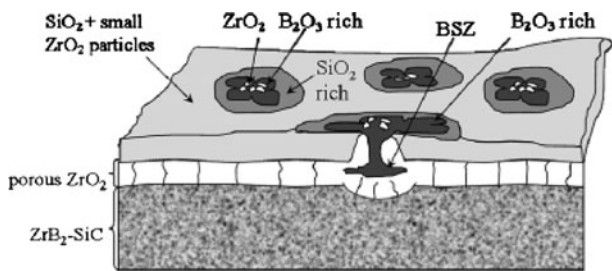


Fig. 4—Schematic of convection cell features on the surface of oxidized  $ZrB_2$ -SiC UHTCs. BSZ is a liquid oxide solution containing boria, silica, and zirconia.<sup>[21]</sup>

The convection cells within the borosilicate liquid result in precipitation of zirconia on the oxidized surface as is shown in Figure 3 and demonstrated schematically in Figure 4.

The amount of SiC must be controlled so that there is sufficient protective glass formed on oxidation. However, if the amount of SiC present is above the percolation threshold, *i.e.*, it is present as an interconnected three-dimensional network, then open channels of porosity remain between the oxide grains when it is oxidized. These will then leave the remaining SiC subject to additional oxidation and lead to a SiC depletion zone. Peng *et al.*<sup>[22]</sup> argued that the SiC depleted zone is the result of a wicking process. The internally formed borosilicate liquid is transported *via* capillary action to the existing borosilicate liquid on the surface formed by earlier oxidation. Increasing the SiC content above the percolation threshold increases the thickness of the SiC depleted zone.<sup>[20]</sup> The SiC depletion zone has also been observed to act as the initiation site for cracking and spallation of material during oxidation at 2173 K (1900 °C).  $ZrB_2$  grains adjacent to the SiC-depleted zones are left exposed to oxygen.<sup>[20]</sup>

The size of the SiC powder particles also has an effect on the properties of the UHTCs. The use of ultrafine

SiC with submicron particle size can produce  $ZrB_2$ -SiC composites that have improved mechanical and thermomechanical properties compared with a material prepared with standard starting powders of much larger particle size.<sup>[23]</sup> This is because of a more uniform particle dispersion that suppresses diboride grain growth resulting in a finer microstructure that is more efficient at crack deflection and bridging. Ultrafine SiC also allows material to be produced by hot pressing at 2173 K (1900 °C) without the presence of a sintering aid<sup>[24]</sup> and improves the oxidation resistance of the material.<sup>[24–27]</sup> The flexural strength of  $ZrB_2$ -SiC composites produced with ultrafine SiC can increase after oxidation, whereas the flexural strength of composites produced with larger SiC powder (average particle size  $\approx 6.4 \mu m$ ) decreases after oxidation.<sup>[26]</sup>

As the temperature is increased, a passive to active transition of SiC oxidation occurs between 1873 K and 1973 K (1600 °C and 1700 °C) in air under atmospheric pressure,<sup>[25,28]</sup> so that above these temperatures, any protection afforded by a glassy oxide layer is largely lost.

### III. OXIDATION KINETICS

Extensive oxidation studies have been performed to determine the oxidation kinetics of  $ZrB_2$  and  $ZrB_2$ -SiC composites.<sup>[4]</sup> For the oxidation of  $ZrB_2$  without SiC, the diffusion of oxygen through the boria glass layer was identified as the rate limiting step up to  $\sim 1473$  K (1200 °C). The protective liquid phase evaporates above this temperature; thus, the oxidation rate becomes dependent on oxygen diffusion through the zirconium oxide layer.

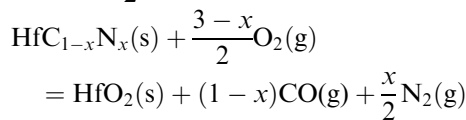
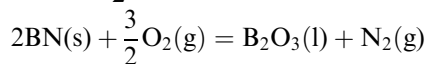
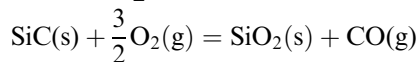
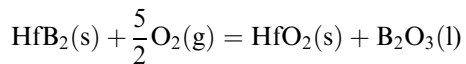
UHTCs containing SiC retain the protective glassy layer for a larger temperature range than those without. However, SiC only improves the oxidation resistance at temperatures above 1623 K (1350 °C), the temperature at which the silicon is oxidized. Below this temperature,



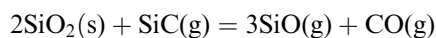
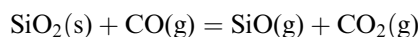
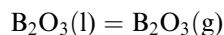
SiC inclusions remain in the oxide layer. Hinze *et al.*<sup>[29]</sup> found that the rate-limiting step accounting for the parabolic kinetics observed in these materials was the diffusion of oxygen through the borosilicate glass; this idea has been supported by more recent research.<sup>[13]</sup>

Monteverde and Bellosi<sup>[13]</sup> studied the oxidation resistance of hot-pressed HfB<sub>2</sub>-SiC composites by isothermal and nonisothermal treatments in air at temperatures ≤1873 K (1600 °C). They found that the oxidation kinetics of the composite fit a parabolic law until partial rupture of the oxide scale occurs, after which the weight gain fits a linear law. The parabolic contribution is a result of the growth of an external oxide scale, which imposes longer diffusion paths progressively on oxygen arriving at the diboride-oxide interface. The negative linear contribution accounts for volatile products (most likely B<sub>2</sub>O<sub>3</sub> or SiO<sub>2</sub>) being released from the outermost borosilicate layer. The HfB<sub>2</sub>-SiC composite also contained HfO<sub>2</sub> and a cubic Hf(C, N) solid solution as secondary phases formed during hot pressing. These had a detrimental effect on the oxidation resistance at temperatures below 1623 K (1350 °C). At temperatures above 1623 K (1350 °C), the SiC improved the oxidation resistance as expected.

While investigating the HfB<sub>2</sub>-SiC material, Monteverde and Bellosi<sup>[13]</sup> suggested the main reactions that described the oxidation process. Depending on the selected temperature range, these reactions involve either mass gain, as follows:



or mass loss, as follows:



For a UHTC material to maintain its oxidation resistance, it must retain the protective oxide layer. Monteverde and Bellosi<sup>[23]</sup> observed rupturing of the oxide scale in a ZrB<sub>2</sub>-SiC ceramic after furnace oxidation testing through several thermal cycles from room temperature to 1973 K (1700 °C). The cracking and spalling of the oxide scale was attributed in part to a phase transformation in the ZrO<sub>2</sub>, which takes place during thermal cycling. At high temperatures, the oxide exists in tetragonal form, whereas at lower temperatures, it exists in monoclinic form. For pure ZrO<sub>2</sub>, the athermal martensitic monoclinic to tetragonal transformation occurs at 1443 K (1170 °C) on heating and 1223 K (950 °C) on cooling.<sup>[30,31]</sup> This is obviously

undesirable for a material that will be subject to thermal cycling with rapid thermal transient conditions. The oxides also have higher coefficients of thermal expansion (CTEs) and lower thermal conductivities than the underlying diboride material. This, coupled with the phase transformation, leads to cracking of the oxide scale, allowing oxidation of the underlying bulk.

At low partial pressures that exist close to the interface between the unreacted bulk and the oxide layer, ZrO<sub>2</sub> forms oxygen lattice vacancies and becomes nonstoichiometric (*i.e.*, ZrO<sub>2-x</sub>). This increases the diffusivity of oxygen through the oxide scale, which also increases oxidation of the underlying bulk.

#### IV. ADDITIVES

The oxidation products of a material formed during exposure to an oxidizing environment are largely responsible for the high-temperature performance of that material. This is determined by the extent to which the oxidized layer can protect the bulk material from subsequent oxidation. The physical and chemical processes that occur at the exposed surface depend on the microstructure and composition of the oxidized material. It follows that modification of the microstructure and composition can have a beneficial (or detrimental) effect on the material's oxidation resistance.

Additives can be used in several ways to improve the oxidation resistance of the UHTCs. The main areas of interest are as follows:

- (a) Increasing viscosity of the borosilicate liquid
- (b) Inhibiting the ZrO<sub>2</sub> polymorphic transformations
- (c) Using alternatives to SiC to introduce silicon
- (d) Forming protective refractory phases at high temperature
- (e) Modifying the microstructure of the ZrO<sub>2</sub> scale

##### A. Increasing Viscosity of the Borosilicate Liquid

Systems with higher viscosity and increased liquidus temperatures inhibit oxygen diffusion to the unreacted bulk, retain the protective liquid at higher temperatures, and suppress evaporation of boria from the glassy phase. Diffusivity is inversely proportional to the viscosity of the liquid through which the diffusion is taking place, which is shown in the Stokes-Einstein relationship<sup>[32]</sup>

$$D = \frac{kT}{6\pi\eta r}$$

where  $D$  is the diffusion constant,  $k$  is Boltzmann's constant,  $T$  is temperature in Kelvin,  $\eta$  is viscosity, and  $r$  is the spherical particle radius.

The viscosity of the borosilicate glass can be increased even more by adding certain elements to the bulk material. The addition of tungsten in 10 and 20 vol pct additions to ZrB<sub>2</sub>-SiC ceramics increased the viscosity of the borosilicate glassy phase significantly but also reduced the material's thermal shock resistance and structural stability at elevated temperatures, which is highly undesirable for sharp, leading-edge materials.<sup>[4]</sup>

The oxidation resistance of hot-pressed  $\text{ZrB}_2 + 25$  vol pct SiC composites has been improved by the addition of diborides of Cr, Ti, Ta, Nb, and V.<sup>[33]</sup> These additions result in the production of the respective oxides in the glass. The improvement in oxidation resistance comes from the fact that borate and silicate glasses containing oxides of the elements listed (Group IV–VI transition metals) are immiscible and lead to phase separation. Such systems contain compositions with high viscosity and liquidus temperatures.<sup>[32]</sup> The immiscibility of the glass increases with increasing cation field strength of the metallic oxide forming element  $z/r^2$  where  $z$  is the valence and  $r$  is the ionic radius.  $\text{ZrB}_2$  ceramics with additions of 10 mol pct  $\text{CrB}_2$ ,  $\text{NbB}_2$ ,  $\text{TaB}_2$ ,  $\text{TiB}_2$ , and  $\text{VB}_2$  had improved oxidation resistance, but most improvement was observed in the  $\text{ZrB}_2$ -SiC + 10 mol pct  $\text{TaB}_2$ , which displayed a weight gain of  $\sim 1.25$  pct after 5 hours of thermogravimetric analysis (TGA) compared with  $\sim 3.5$  pct for the  $\text{ZrB}_2$ -SiC material with no additives.<sup>[33]</sup> The order in which the oxidation resistance was improved correlated well with the cation field strength of the modifying additive.

Opila *et al.*<sup>[11]</sup> investigated the effect of tantalum additions on the oxidation performance of zirconium diboride. They found that the addition of  $\text{TaSi}_2$  improved the oxidation resistance of a  $\text{ZrB}_2 + 20$  vol pct SiC composite. The oxidation rate was reduced by a factor of 10 at 1900 K (1627 °C). They concluded that more research was required to confirm that the improvement in oxidation was a result of the tantalum addition and not from the accompanying increase in silicon. It was suggested that the introduction of Ta resulted in immiscibility of the liquid formed on oxidation, which increased the viscosity of the liquid phase, providing a protective layer that was more resistant to volatilization. Evidence of glass immiscibility on the surface of  $\text{ZrB}_2 + 20$  vol pct SiC-20 vol pct  $\text{TaSi}_2$  after oxidation in air at 1900 K (1627 °C) for 100 minutes is shown in Figure 5.

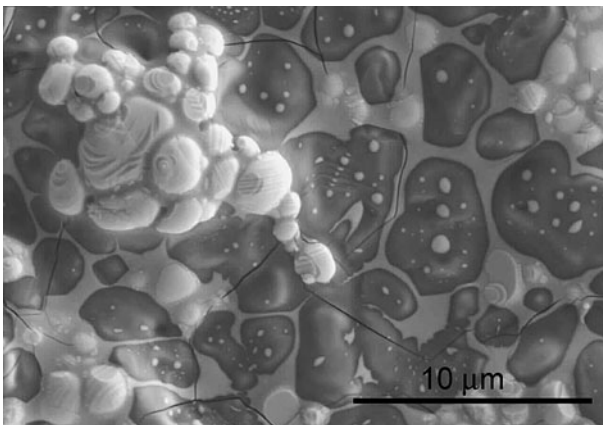


Fig. 5—SEM backscattered image showing evidence of glass immiscibility on the surface of  $\text{ZrB}_2 + 20$  vol pct SiC-20 vol pct  $\text{TaSi}_2$  after oxidation in air at 1900 K (1627 °C) for 100 min. Bright contrast phase is  $\text{ZrO}_2$ , intermediate contrast phase is silicate glass with impurities and dark phase is  $\text{SiO}_2$ .<sup>[11]</sup>

Peng and Speyer<sup>[34]</sup> investigated the effect of  $\text{TaSi}_2$  and  $\text{TaB}_2$  on the oxidation resistance of  $\text{ZrB}_2$ - $\text{B}_4\text{C}$ -SiC composites across the temperature range 1423 K to 1823 K (1150 °C to 1550 °C). The addition of Ta-containing compounds improved the oxidation resistance of the materials over the entire temperature range studied, but the  $\text{TaSi}_2$  performed better than the  $\text{TaB}_2$  presumably because of the ability to form larger amounts of protective silica-based liquid. Peng *et al.*<sup>[22]</sup> investigated the effect of SiC,  $\text{TaB}_2$ , and  $\text{TaSi}_2$  on the isothermal oxidation resistance of  $\text{ZrB}_2$ . They found that an increase in SiC decreased the thickness of both the silica-rich glassy layer and the SiC depletion zone.  $\text{TaB}_2$  was more effective at improving the oxidation performance than  $\text{TaSi}_2$ . Both caused improvements thought to be a result of the formation of a zirconium-tantalum boride solid solution. After oxidation of the solid solution, segregated  $\text{ZrO}_2$  and TaC phases form, resulting in finer particles ( $\sim 1 \mu\text{m}$ ) present in the liquid phase than with oxidation of pure  $\text{ZrB}_2$ . The finer particles are more effective at trapping the liquid phase in the  $\text{ZrO}_2$  layer and preventing oxygen transport through the liquid. The additives were effective only at small concentrations ( $\sim 3.32$  mol pct) and at larger concentrations were detrimental to the oxidation resistance because of the formation of zirconia dendrites, which act as conduits for oxygen transport into the bulk.

The addition of yttria has been investigated by several groups. Zhang *et al.*<sup>[35]</sup> found that adding 3 vol pct improved sinterability of the powders and suppressed grain growth by reacting with oxides on the starting powder surfaces. Grain size refinement improved the fracture toughness and flexural strength of the material. Adding  $\text{LaB}_6$  to a  $\text{ZrB}_2 + 20$  vol pct SiC UHTC<sup>[36]</sup> resulted in significantly higher fracture toughness compared with the same UHTC without the  $\text{LaB}_6$  (5.7 MPa  $\text{m}^{1/2}$  and 4.0 to 4.8 MPa  $\text{m}^{1/2}$ , respectively) because of enhanced crack deflection and bridging near SiC particles.  $\text{MoSi}_2$  has a beneficial effect on the mechanical and oxidation properties of  $\text{ZrB}_2$ -SiC ceramics and is an effective sintering aid for  $\text{ZrB}_2$ -SiC UHTCs produced by hot pressing<sup>[15,37]</sup> and spark plasma sintering.<sup>[38]</sup> Zhang *et al.*<sup>[37]</sup> found that additions of tungsten carbide improved the oxidation resistance of pressureless sintered  $\text{ZrB}_2$  at 1873 K (1600 °C) by forming a solid solution with the  $\text{ZrB}_2$ , which allowed liquid phase sintering of the  $\text{ZrO}_2$  formed during oxidation. This process resulted in a substantial decrease in oxide scale thickness in the WC-containing ceramic.

### B. Inhibiting the $\text{ZrO}_2$ Polymorphic Transformations

The integrity of the oxide scale can be improved by inhibiting the  $\text{ZrO}_2$  polymorphic transformations and their associated volume changes. In low temperature systems, this is achieved by the addition of stabilizing cations such as Mg, Ca, and Y. However, these cations are lost from the  $\text{ZrO}_2$  lattice at relatively low temperatures, and for UHTCs, alternative cations have been sought. The addition of a cation such as Ta results in substitution of the cation on the Zr site in  $\text{ZrO}_2$ , thus reducing the concentration of oxygen vacancies because

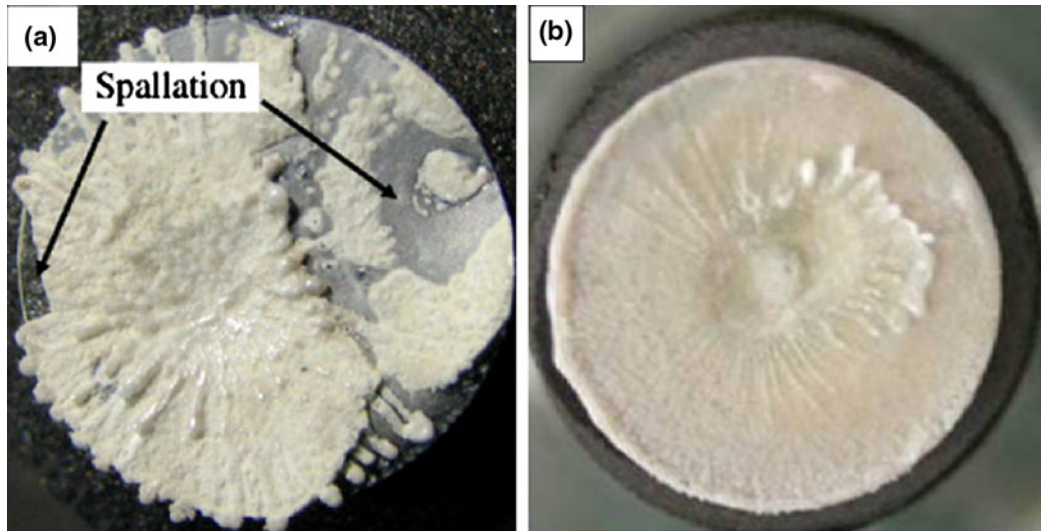


Fig. 6—Photographs of (a) ZrB<sub>2</sub>-20 vol pct SiC and (b) ZrB<sub>2</sub>-20 vol pct SiC-10 vol pct LaB<sub>6</sub> after oxyacetylene torch testing at 2673 K (2400 °C) for 600 s.<sup>[43]</sup>

of the higher valence of the cation (Ta forms Ta<sub>2</sub>O<sub>5</sub> when oxidized). This decreases oxygen diffusion through the scale and stabilizes the oxide phase, increasing adhesion of the scale to the bulk ZrB<sub>2</sub>-SiC material. The cation must be of higher valence and must form a refractory oxide scale. In addition to this, candidate additives must be introduced as a refractory phase and form a refractory oxide. The two best candidates are those based on niobium and tantalum, but tantalum is preferable as Ta<sub>2</sub>O<sub>5</sub> has a melting temperature of 2153 K (1880 °C) (compared with 1793 K [1520 °C] for Nb<sub>2</sub>O<sub>5</sub>).<sup>[33]</sup> Tantalum can be added in elemental form or as a carbide, boride, or silicide. The formation of intermediate phases should be considered. For instance, the addition of Ta<sub>2</sub>O<sub>5</sub> could form Ta<sub>2</sub>O<sub>5</sub>·6ZrO<sub>2</sub> with ZrO<sub>2</sub>. This phase has a lower melting temperature than the pure oxides and could have a beneficial or detrimental effect on the oxidation behavior of the composite.

### C. Using Alternatives to SiC to Introduce Silicon

Alternative methods of introducing Si to the system have been investigated. Ceramics in the system ZrB<sub>2</sub>-Ta<sub>5</sub>Si<sub>3</sub> have been investigated, as Ta<sub>5</sub>Si<sub>3</sub> has a higher melting point than SiC (2773 K and 1573 K [2500 °C and 2300 °C], respectively). Ta<sub>5</sub>Si<sub>3</sub> provides the tantalum to induce glass immiscibility and silicon to form the protective borosilicate glass in the oxidized layer.<sup>[39]</sup> ZrB<sub>2</sub>- and HfB<sub>2</sub>-TaSi<sub>2</sub> composites have been formed by hot pressing,<sup>[40]</sup> resulting in formation of a solid solution as the tantalum entered the boride matrix. The HfB<sub>2</sub>-TaSi<sub>2</sub> displayed superior mechanical properties to the ZrB<sub>2</sub>-based material. The substitution of Ti for SiC (*e.g.*, a Zr-B-Ti system) has been suggested for making an alternative UHTC system because of the significantly reduced vaporization rate displayed by TiO<sub>2</sub> compared with SiO<sub>2</sub>.<sup>[41]</sup>

### D. Forming Protective Refractory Phases at High Temperature

Research into the introduction of additives to ZrB<sub>2</sub>-SiC ceramics largely focuses on using the additives to alter the properties of the liquid phase formed at oxidation. A different approach is to use additives to form a solid refractory scale at high temperatures, which can resist oxidation at higher temperatures than the original material, thus providing effective protection to the underlying bulk and preventing subsequent oxidation. Candidate additives for this approach include those based on rare earth elements, in particular those containing lanthanum.

Originally, zirconium diboride was investigated as an additive to improve the oxidation resistance of LaB<sub>6</sub> and was found to be effective up to ~1573 K (1300 °C).<sup>[42]</sup> Zhang *et al.*<sup>[43]</sup> prepared hot-pressed ZrB<sub>2</sub>-20 vol pct SiC-10 vol pct LaB<sub>6</sub> and compared the oxidation performance with a ZrB<sub>2</sub>-20 vol pct SiC ceramic by oxidizing both materials with an oxyacetylene torch. Both samples underwent oxidation up to 2673 K (2400 °C), and the ceramic with the LaB<sub>6</sub> addition displayed significantly less spalling and cracking than the ZrB<sub>2</sub>-SiC sample (Figure 6). Also, the weight changes for the ZrB<sub>2</sub>-SiC-LaB<sub>6</sub> and ZrB<sub>2</sub>-SiC were 0.2 pct and 3.1 pct, respectively.

An energy-dispersive X-ray analysis of the oxidized surfaces showed that the LaB<sub>6</sub>-containing sample had formed an oxidized layer containing *m*-ZrO<sub>2</sub>, *t*-ZrO<sub>2</sub>, La<sub>2</sub>O<sub>3</sub>, and La<sub>2</sub>Zr<sub>2</sub>O<sub>7</sub>. The addition of LaB<sub>6</sub> not only impeded the tetragonal to monoclinic ZrO<sub>2</sub> transformation on cooling but also formed a self-generating oxidation barrier containing lanthanum zirconate, which has a significantly higher melting temperature than SiC. The elemental maps showed that both silica and boron are no longer present in the outer oxide layer after oxidation at ~2673 K (2400 °C), but the lanthanum additions have been retained in a compact scale on the oxidized surface.



Lanthanum has also been added to a  $ZrB_2$ -SiC material as  $La_2O_3$ ,<sup>[44]</sup> but resulted in the formation of an amorphous grain boundary phase and substantial  $ZrB_2$  and SiC grain growth. The same work found that additions of other rare earth oxides ( $Y_2O_3$  and  $Yb_2O_3$ ) had beneficial effects on the densification, hardness, and fracture toughness of the  $ZrB_2$ -SiC but did not investigate their effect on oxidation resistance.

Jayaseelan<sup>[45]</sup> investigated the addition of several rare earth (RE)-containing compounds to  $ZrB_2 + 20$  vol pct SiC. Samples were prepared with 10 vol pct  $LaB_6$ ,  $La_2O_3$ , or  $Gd_2O_3$  and underwent oxidation testing at 1873 K (1600 °C). All samples successfully formed a thick (>100  $\mu m$ ), dense layer of  $RE_2Zr_2O_7$  during oxidation (Figure 7). These zirconates have melting temperatures >2573 K (2300 °C) and will provide oxidation protection at temperatures when the borosilicate phase has vaporized from the exposed surface. Also, the reaction of the RE with  $ZrO_2$  is expansive and therefore fills voids at the oxidized surface created by the removal of volatile species such as  $B_2O_3$ .

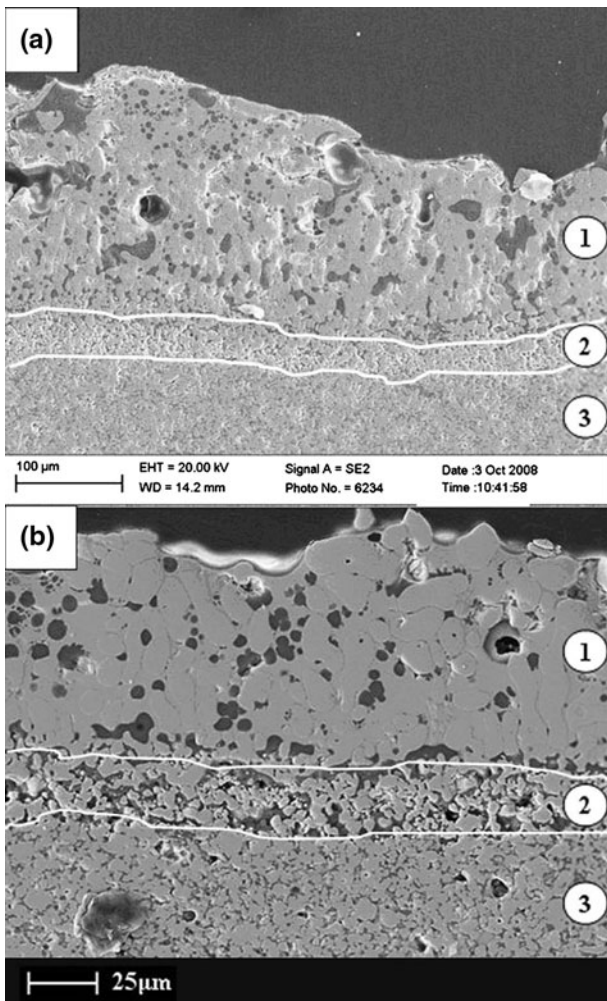


Fig. 7—Secondary electron micrographs of oxidized scale on (a)  $ZrB_2$ -20 vol pct SiC-10 vol pct  $La_2O_3$  and (b)  $ZrB_2$ -20 vol pct SiC-10 vol pct  $LaB_6$  after oxidation for 1 h at 1873 K (1600 °C) showing (1) dense La-containing layer, (2) intermediate  $ZrO_2$ -containing layer, and (3) unreacted bulk.<sup>[45]</sup>

### E. Modifying the Microstructure of the $ZrO_2$ Scale

Another novel technique is the use of additives to alter the microstructure of the  $ZrO_2$  scale. By providing a liquid phase sintering route for the  $ZrO_2$ , it is possible to decrease the porosity of the scale and inhibit the subsequent transport of oxygen into the bulk material. As  $ZrO_2$  has a melting point of 2988 K (2715 °C), a sufficiently dense scale would provide effective oxidation resistance at temperatures above those at which the boria or borosilicate phase is vaporized (~1873 K [1600 °C]). This approach has been investigated by Zhang *et al.*<sup>[46]</sup> with additions of W to  $ZrB_2$ , which results in formation of a  $WO_3$ - $ZrO_2$  eutectic at ~1548 K (1275 °C).  $ZrB_2 + 4$  mol pct WC ceramics underwent TGA at 10 deg/min to 1773 K (1500 °C) and isothermal oxidation studies at 1773 K or 1873 K (1500 °C or 1600 °C) for 1, 2, or 3 hours in flowing air. The  $ZrB_2 + 4$  mol pct WC had better oxidation resistance than  $ZrB_2$ , as indicated by the normalized mass gain after TGA heating to 1773 K (1500 °C) (~4.5 mg/cm<sup>2</sup> and ~14 mg/cm<sup>2</sup>, respectively).  $ZrB_2 + WC$  also showed superior oxidation resistance in the isothermal oxidation tests at 1773 K and 1873 K (1500 °C and 1600 °C), and the reduced mass gain of the  $ZrB_2 + WC$  samples was more significant at longer oxidation times, supporting densification of the  $ZrO_2$  scale. The addition of WC to  $ZrB_2$ -SiC ceramics was also investigated and the presence of W increased the oxidation resistance of these ceramics as well. However, additional research is necessary to confirm that the improved oxidation resistance is caused by liquid phase sintering of the  $ZrO_2$  scale.

## V. DENSIFICATION METHODS

The conventional method for densifying UHTCs is hot pressing, performed either with or without sintering additives. Significant research has examined alternative processing routes for UHTCs to reduce processing times and temperatures and, therefore, reduce the cost associated with the techniques. Some of these alternative techniques also improve the oxidation resistance of the material.

The presence of secondary phases in the microstructure has a detrimental effect on the material high-temperature capability by introducing grain boundary phases, which can have lower melting temperatures and provide routes for oxygen diffusion into the material. The presence of oxygen impurities can be detrimental to the densification ability of the starting powder or cause rapid grain growth; it also contributes to the formation of secondary phases. Nitrides and reducing additives have been added to the powders to enhance sinterability,<sup>[23,47–49]</sup> but these additives introduce secondary phases to the material.

The main production techniques used for formation of UHTC materials are as follows:

- (a) Hot pressing
- (b) Pressureless sintering
- (c) Self-propagating high-temperature synthesis (SHS)
- (d) Reactive hot pressing (RHP)
- (e) Spark-plasma sintering (SPS)

### A. Hot Pressing

Hot pressing is the conventional method for fabricating UHTCs and has been used extensively,<sup>[8–10,12,16,17,20,22,27,33,35,39,47,48,50–65]</sup> with typical temperatures of ~2173 K (1900 °C) and applied pressures between 30 and 50 MPa. It allows full densification without the use of sintering aids, although most research employs modest amounts of sintering aids such as silicides, borides, metals (*e.g.*, Ni), or C to reduce processing times and temperatures, thus reducing the costs associated with the production technique.

Monteverde *et al.*<sup>[66]</sup> have performed extensive research using hot pressing and various sintering aids. A monolithic ZrB<sub>2</sub> ceramic was compared with ZrB<sub>2</sub>-TiB<sub>2</sub> and ZrB<sub>2</sub>-B<sub>4</sub>C composites, and it was concluded that the composite materials had better mechanical properties and performed better in long-term furnace oxidation tests. Full densification of a HfB<sub>2</sub> + 30 vol pct SiC ceramic was obtained by hot pressing at 2173 K (1900 °C) for 35 minutes using 2 vol pct TaSi<sub>2</sub> as a sintering aid.<sup>[67]</sup>

### B. Pressureless Sintering

The refractory nature of ZrB<sub>2</sub> makes it difficult to sinter, and in general, pressureless sintering requires the presence of more sintering aids than other firing techniques. As a consequence, pressureless sintered material often contains amorphous phases that can be detrimental to the high-temperature capability of the material. Chamberlain *et al.*<sup>[68]</sup> produced a ZrB<sub>2</sub> ceramic without sintering aids that reached 98 pct theoretical density but required 9 hours pressureless sintering at 2423 K (2150°C). Fahrenholtz *et al.*<sup>[69]</sup> found that ZrB<sub>2</sub> could not be sintered pressurelessly without the presence of a sintering aid (in this case a combination of B<sub>4</sub>C and C), which reacts with and removes oxygen impurities from the surface of the diboride powders. A ~100 pct dense material was formed at 2173 K (1900 °C) with B<sub>4</sub>C and C present as sintering aids.

### C. Self-Propagating High Temperature Synthesis

SHS is not a densification method but uses solid-state combustion to produce materials by using internally generated chemical energy from exothermic reactions. The characteristics of this method include fast reaction times, low energy requirements, simple experimental apparatus, and high-purity products. A disadvantage is that the reactions are difficult to control.

SHS can also be used to prepare ZrB<sub>2</sub> powders using inexpensive raw materials.<sup>[70]</sup> When used for the production of powders, the high heating and cooling rates involved are thought to introduce planar defects, such as stacking faults, and linear defects such as dislocations whose associated strain fields increase the sinterability of the powders by providing a driving force for rearrangement of atoms. ZrB<sub>2</sub> powders can be formed by SHS using zirconium and boron.<sup>[71]</sup> The powders are dry mixed and cold pressed to form pellets. The pellets are ignited and the process is an explosive one accompanied

by a large gas release. As a consequence, the resulting material is too fragile to be used as a bulk material, although X-ray diffraction indicates it is ZrB<sub>2</sub>.

SHS has several advantages over conventional hot pressing of UHTCs, such as control of exaggerated grain growth and lower processing temperatures. However, several problems with hot pressed materials have been overcome by addition of reinforcing phases and refinement of starting powder size.

### D. Reactive Hot Pressing

To avoid the expensive processing conditions of hot pressing, RHP can be used as an alternative production route. RHP involves *in situ* high-temperature, solid-state chemical displacement reactions. This has the benefit of controlling the microstructure and producing chemically compatible, evenly distributed phases. The main advantage of RHP compared with SHS from a processing point of view is that the displacement reactions can take place at much lower temperatures than those that occur during SHS. The heating rate during reactive hot pressing must be sufficiently slow (~10 °C/min) to prevent spontaneous self-combustion.

Monteverde<sup>[72]</sup> fabricated a HfB<sub>2</sub>-SiC composite by reactive hot pressing. Solid reagents (Hf/Si/B<sub>4</sub>C) were mixed mechanically, converted into the basic components (HfB<sub>2</sub> and SiC), and hot pressed directly at 2173 K (1900 °C) to achieve full density. The composite exhibited comparable physical properties to conventionally hot pressed material. Wu *et al.*<sup>[14]</sup> produced a ZrB<sub>2</sub>-SiC-ZrC composite from a mixture of zirconium, silicon, and B<sub>4</sub>C by reactive hot pressing at 2073 K (1800 °C) for 60 minutes under 20 MPa in an argon atmosphere. The microstructure was not homogeneous; it contained residual porosity and large ZrB<sub>2</sub> grains (up to 10- $\mu$ m diameter) because of the relatively large size of the starting powder ( $\leq 25$ - $\mu$ m particle size). These problems could be rectified by improving the uniformity of mixing and using starting powders with smaller particle size. The starting powder size and morphology has a strong effect on the microstructure in RHP ceramics. Qiang *et al.*<sup>[73]</sup> formed a fully dense ZrB<sub>2</sub>-SiC-ZrC composite successfully at 2173 K (1900 °C) by RHP. The microstructure was fine grained (~1  $\mu$ m), resulting in high values of flexural strength (526  $\pm$  9 MPa) and fracture toughness (6.50  $\pm$  0.30 MPa m<sup>1/2</sup>). Wu *et al.*<sup>[74]</sup> fabricated a ZrB<sub>2</sub>-SiC-ZrC composite by RHP at 2073 K (1800 °C)<sup>[14]</sup> and another at 1873 K (1600 °C), which reached theoretical densities of 96.8 pct and 97.3 pct, respectively. The material sintered at 1873 K (1600°C) displayed mechanical properties comparable to those previously reported for materials that had experienced higher sintering temperatures. Rangaraj *et al.*<sup>[75,76]</sup> found that nonstoichiometric ZrC<sub>x</sub> played a crucial role in RHP of Zr-B<sub>4</sub>C powder mixtures at 1473 K (1200 °C) and in ZrB<sub>2</sub>-SiC composites produced at 1873 K (1600 °C).

Zhang and Zhang<sup>[62]</sup> compared the effect of processing method on microstructure by examining ZrB<sub>2</sub>-SiC-ZrC composites that had been formed by RHP and hot



pressing. The hot-pressed material had equiaxed  $ZrB_2$  grains, whereas the RHP material had equiaxed and plate-like  $ZrB_2$  grains. This difference in microstructure had an effect on the mechanical properties of the materials: The HP material had higher flexural strength ( $681 \pm 67$  MPa compared with  $654 \pm 17$  MPa for the RHP material), whereas the RHP material exhibited more effective toughening mechanisms.

### E. Spark-Plasma Sintering

SPS, which is also known as the field-assisted sintering technique or pulsed electrical current sintering, is an unconventional method for consolidating powders with relatively poor sinterability in short times. SPS uses conventional resistance heating and pressure but also pulses a direct current through the graphite die (and powder if it is electrically conducting), which is shown schematically in Figure 8. The pulsed current enhances grain boundary diffusion and migration, which increases the final density of the ceramic by eliminating closed porosity.

SPS has been shown to provide a processing route for these highly refractory materials that does not require sintering aids and produces fully dense products at lower temperatures and in shorter times than conventional hot pressing.<sup>[78,79]</sup> This has the effect of maintaining a fine grain size, which is beneficial to the mechanical properties of the material such as fracture toughness. The technique has been particularly successful when using starting powders fabricated using an SHS method.<sup>[79]</sup>

Several researchers<sup>[78]</sup> have produced dense UHTCs successfully by SPS without sintering aids using sintering temperatures in the range of 2173 K to 2373 K (1900 °C to 2100 °C) and holding times on the order of minutes. Materials produced by SPS have displayed comparable and/or improved mechanical properties and oxidation resistance when compared with hot-pressed materials. The reason for the superior oxidation

resistance may be the removal of surface oxides during sintering. The storage and processing of  $ZrB_2$  (and  $HfB_2$ ) in air results in the formation of surface oxides on the powder particles.<sup>[51]</sup> These surface oxides not only inhibit the sinterability of the diboride, but also they introduce oxides such as  $B_2O_3$  into the bulk material. The presence of these low-melting-point oxides has a detrimental effect on the high-temperature mechanical properties and oxidation resistance. The pulsed electrical current used during SPS is thought to cause thermal or electrical decomposition of insulating surface oxides,<sup>[80,81]</sup> although the process by which the SPS method achieves this and the rapid sintering rates is not yet understood fully.

The parameters of the SPS technique can be altered to produce materials with fine microstructures, which tend to contain fewer secondary phases than materials produced by conventional methods. SPS materials can be produced using sintering aids<sup>[82]</sup> and still have superior oxidation resistance than hot-pressed materials.

## VI. CONCLUSIONS

There are many methods to improve oxidation resistance in UHTCs, but they can be detrimental to other material properties or only provide improvements over limited temperature ranges. By controlling the starting powder size and additives, employing efficient mixing techniques and using production methods that minimize secondary phase formation, it is possible to improve the oxidation resistance. Even so, current research is still far from producing a material that is reliable and can be used repeatedly in extreme environments. The modification of the glass composition is limited to the fact that however viscous the liquid phase is during exposure to ultra high temperature environments, the materials still need to resist the concurrent shear forces experienced. It may be that the way in which we achieve improved oxidation resistance in UHTCs for high-temperature use will require an entirely new direction, but to date, UHTCs that produce self-generating refractory oxidation barriers or dense  $ZrO_2$  scales show the greatest promise and might provide the solution to the ongoing search for UHTC materials.

## REFERENCES

1. M.J. Gasch, D.T. Ellerby, and S.M. Johnson: *Handbook of Ceramic Composites*, Springer, New York, NY, 2004, p. 558.
2. K. Upadhyaya, J.M. Yang, and W.P. Hoffman: *Am. Ceram. Soc. Bull.*, 1997, vol. 76, pp. 51–56.
3. W.G. Fahrenholtz, G.E. Hilmas, I.G. Talmy, and J.A. Zaykoski: *J. Am. Ceram. Soc.*, 2007, vol. 90, pp. 1347–64.
4. M.M. Opeka, I.G. Talmy, and J.A. Zaykoski: *J. Mater. Sci.*, 2004, vol. 39, pp. 5887–5904.
5. E. Wuchina, E. Opila, M.M. Opeka, W. Fahrenholtz, and I. Talmy: *Electrochem. Soc. Interf.*, 2007, vol. 16, pp. 30–36.
6. A.K. Kuriakosem and J.L. Margrave: *J. Electrochem. Soc.*, 1964, vol. 111, pp. 827–31.
7. J.B. Berkowitz-Mattuck: *J. Electrochem. Soc.*, 1966, vol. 113, pp. 908–14.
8. Q. Liu, W. Han, X. Zhang, S. Wang, and J. Han: *Mater. Lett.*, 2009, vol. 63, pp. 1323–25.

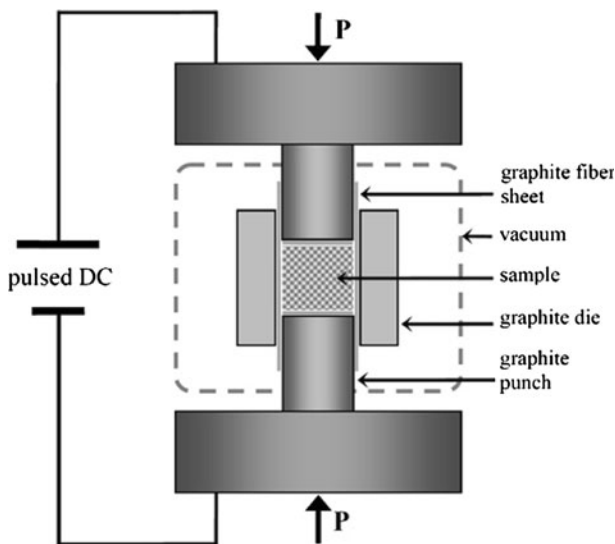


Fig. 8—Schematic of SPS equipment.<sup>[77]</sup>

9. M.M. Opeka, I.G. Talmy, E.J. Wuchina, J.A. Zaykoski, and S.J. Causey: *J. Eur. Ceram. Soc.*, 1999, vol. 19, pp. 2405–14.
10. S.R. Levine, E. Opila, M.C. Halbig, J.D. Kiser, M. Singh, and J.A. Salem: *J. Eur. Ceram. Soc.*, 2002, vol. 22, pp. 2757–67.
11. E. Opila, S. Levine, and J. Lorincz: *J. Mater. Sci.*, 2004, vol. 39, pp. 5969–77.
12. W. Fahrenholtz, G.E. Hilmas, A.L. Chamberlain, and J.W. Zimmermann: *J. Mater. Sci.*, 2004, vol. 39, pp. 5951–57.
13. F. Monteverde and A. Bellosi: *J. Eur. Ceram. Soc.*, 2005, vol. 25, pp. 1025–31.
14. W. Wu, G. Zhang, Y. Kan, and P. Wang: *J. Am. Ceram. Soc.*, 2006, vol. 89, pp. 2967–69.
15. F. Monteverde: *Mater. Chem. Phys.*, 2009, vol. 113, pp. 626–33.
16. F. Monteverde and A. Bellosi: *J. Electrochem. Soc.*, 2003, vol. 150, pp. 552–59.
17. M. Gasch, D. Ellerby, I. Irby, S. Beckman, M. Gusman, and S. Johnson: *J. Mater. Sci.*, 2004, vol. 39, pp. 5925–37.
18. A. Rezaie, W.G. Fahrenholtz, and G.E. Hilmas: *J. Eur. Ceram. Soc.*, 2007, vol. 27, pp. 2495–2501.
19. J. Li, T.J. Lenosky, C.J. Först, and S. Yip: *J. Am. Ceram. Soc.*, 2008, vol. 91, pp. 1475–80.
20. X. Zhang, P. Hu, and J. Han: *J. Mater. Res.*, 2008, vol. 23, pp. 1961–72.
21. S.N. Karlsdottir and J.W. Halloran: *J. Am. Ceram. Soc.*, 2008, vol. 91, pp. 3652–58.
22. F. Peng, Y. Berta, and R.F. Speyer: *J. Mater. Res.*, 2009, vol. 24, pp. 1855–67.
23. F. Monteverde and A. Bellosi: *Solid State Sci.*, 2005, vol. 7, pp. 622–30.
24. F. Monteverde: *Appl. Phys. Mater. Sci. Process.*, 2006, vol. 82, pp. 329–37.
25. J. Wang, L. Zhang, Q. Zeng, G.L. Vignoles, and A. Guette: *J. Am. Ceram. Soc.*, 2008, vol. 91, pp. 1665–73.
26. S. Guo, J. Yang, H. Tanaka, and Y. Kagawa: *Compos. Sci. Technol.*, 2008, vol. 68, pp. 3033–40.
27. S.S. Hwang, A.L. Vasiliev, and N.P. Padture: *Mater. Sci. Eng. A*, 2007, vol. A464, pp. 216–24.
28. M.J. Balat: *J. Eur. Ceram. Soc.*, 1996, vol. 16, pp. 55–62.
29. J.W. Hinze, W.C. Tripp, and H.C. Graham: *J. Electrochem. Soc.*, 1975, vol. 122, pp. 1249–54.
30. X. Jin: *Curr. Opin. Solid State Mater. Sci.*, 2005, vol. 9, pp. 313–18.
31. C. Wang, M. Zinkevich, and F. Aldinger: *J. Am. Ceram. Soc.*, 2006, vol. 89, pp. 3751–58.
32. D.R. Uhlmann and N.J. Kreidl: *Glass: Science and Technology, vol. 3: Viscosity and Relaxation*, Academic Press, New York, NY, 1986, p. 412.
33. I.G. Talmy, J.A. Zaykoski, M.M. Opeka, and S. Dallek: *High Temperature Corrosion and Materials Chemistry III*, 2001, vol. 2001, pp. 144–58.
34. F. Peng and R.F. Speyer: *J. Am. Ceram. Soc.*, 2008, vol. 91, pp. 1489–94.
35. X. Zhang, X. Li, J. Han, W. Han, and C. Hong: *J. Alloys Compd.*, 2008, vol. 465, pp. 506–11.
36. A. Spring, W. Guo, G. Zhang, P. Wang, and V.D. Krstic: *J. Am. Ceram. Soc.*, 2008, vol. 91, pp. 2763–65.
37. X. Zhang, Q. Qu, J. Han, W. Han, and C. Hong: *Scripta Mater.*, 2008, vol. 59, pp. 753–56.
38. D. Sciti, L. Silvestroni, and M. Nygren: *J. Eur. Ceram. Soc.*, 2008, vol. 28, pp. 1287–96.
39. I.G. Talmy, J.A. Zaykoski, M.M. Opeka, and A.H. Smith: *J. Mater. Res.*, 2006, vol. 21, pp. 2593–99.
40. D. Sciti, L. Silvestroni, G. Celotti, C. Melandri, and S. Guicciardi: *J. Am. Ceram. Soc.*, 2008, vol. 91, pp. 3285–91.
41. J.C.A. Bronson: *J. Am. Ceram. Soc.*, 2008, vol. 91, pp. 1448–52.
42. R. Gao, G. Min, H. Yu, S. Zheng, Q. Lu, J. Han, and W. Wang: *Ceram. Int.*, 2005, vol. 31, pp. 15–19.
43. X. Zhang, P. Hu, J. Han, L. Xu, and S. Meng: *Scripta Mater.*, 2007, vol. 57, pp. 1036–39.
44. W. Guo, J. Vleugels, G. Zhang, P. Wang, and O. Van der Biest: *J. Eur. Ceram. Soc.*, 2009, vol. 29, pp. 3063–68.
45. D.D. Jayaseelan: unpublished research, Imperial College London, 2010.
46. S. Zhang, W. Fahrenholtz, and G.E. Hilmas: *ECS Trans.*, 2009, vol. 16, p. 137.
47. F. Monteverde and A. Bellosi: *Adv. Eng. Mater.*, 2003, vol. 5, pp. 508–12.
48. F. Monteverde and A. Bellosi: *Scripta Mater.*, 2002, vol. 46, pp. 223–28.
49. S. Zhang, G.E. Hilmas, and W.G. Fahrenholtz: *J. Am. Ceram. Soc.*, 2006, vol. 89, pp. 1544–50.
50. A. Rezaie, W.G. Fahrenholtz, and G.E. Hilmas: *J. Mater. Sci.*, 2007, vol. 42, pp. 2735–44.
51. A. Bellosi, F. Monteverde, D.D. Fabbri, and C. Melandri: *J. Mater. Process. Manuf. Sci.*, 2000, vol. 9, pp. 156–70.
52. J.J. Melendez-Martinez, A. Dominguez-Rodriguez, F. Monteverde, C. Melandri, and G. de Portu: *J. Am. Ceram. Soc.*, 2002, vol. 22, pp. 2543–49.
53. F. Monteverde, S. Guicciardi, and A. Bellosi: *Mater. Sci. Eng. A*, 2003, vol. 346, pp. 310–19.
54. F. Monteverde and A. Bellosi: *Solid State Sci.*, 2005, vol. 7, pp. 622–30.
55. V. Medri, F. Monteverde, A. Balbo, and A. Bellosi: *Adv. Eng. Mater.*, 2005, vol. 7, pp. 159–63.
56. D. Sciti, F. Monteverde, S. Guicciardi, G. Pezzotti, and A. Bellosi: *Mater. Sci. Eng. A*, 2006, vol. 434, pp. 303–09.
57. D. Sciti, L. Silvestroni, and A. Bellosi: *J. Mater. Res.*, 2006, vol. 21, pp. 1460–66.
58. W. Li, X. Zhang, C. Hong, J. Han, and W. Han: *Mater. Sci. Eng. A*, 2008, vol. A494, p. 147.
59. F. Monteverde, A. Bellosi, and L. Scatteia: *Mater. Sci. Eng. A*, 2008, vol. A485, pp. 415–21.
60. X. Zhang, Z. Wang, X. Sun, W. Han, and C. Hong: *Mater. Lett.*, 2008, vol. 62, pp. 4360–62.
61. X. Zhang, P. Hu, J. Han, and S. Meng: *Compos. Sci. Technol.*, 2008, vol. 68, pp. 1718–26.
62. X. Zhang and X. Zhang: *Scripta Mater.*, 2008, vol. 59, pp. 753–56.
63. J.W. Zimmermann, G.E. Hilmas, and W.G. Fahrenholtz: *J. Am. Ceram. Soc.*, 2008, vol. 91, pp. 1405–11.
64. J.W. Zimmermann, G.E. Hilmas, and W.G. Fahrenholtz: *Mater. Chem. Phys.*, 2008, vol. 112, pp. 140–45.
65. S. Lee and D. Kim: *Key Eng. Mater.*, 2009, vol. 403, pp. 253–55.
66. F. Monteverde, A. Bellosi, and S. Guicciardi: *J. Eur. Ceram. Soc.*, 2002, vol. 22, pp. 279–88.
67. F. Monteverde: *J. Alloys Compd.*, 2007, vol. 428, pp. 197–205.
68. A.L. Chamberlain, W.G. Fahrenholtz, and G.E. Hilmas: *J. Am. Ceram. Soc.*, 2006, vol. 89, pp. 450–56.
69. W.G. Fahrenholtz, G.E. Hilmas, S. Zhang, and S. Zhu: *J. Am. Ceram. Soc.*, 2008, vol. 91, pp. 1398–1404.
70. A.K. Khanra, L.C. Pathak, S.K. Mishra, and M.M. Godkhindi: *J. Mater. Sci. Lett.*, 2003, vol. 22, pp. 1189–91.
71. N. Bertolino, M. Monagheddu, A. Tacca, P. Giuliani, C. Zanotti, F. Maglia, and U.A. Tamburini: *J. Mater. Res.*, 2003, vol. 18, pp. 448–55.
72. F. Monteverde: *Compos. Sci. Technol.*, 2005, vol. 65, pp. 1869–79.
73. Q. Qiang, X. Zhang, S. Meng, W. Han, C. Hong, and J. Han: *Mater. Sci. Eng. A*, 2008, vol. 491, pp. 117–23.
74. W. Wu, G.J. Zhang, Y.M. Khan, and P.L. Wang: *J. Am. Ceram. Soc.*, 2008, vol. 91, pp. 2501–08.
75. L. Rangaraj, S.J. Suresha, C. Divakar, and V. Jayaram: *Metall. Mater. Trans. A*, 2008, vol. 39A, pp. 1495–1505.
76. L. Rangaraj, C. Divakar, and V. Jayaram: *J. Eur. Ceram. Soc.*, 2010, vol. 30, pp. 129–38.
77. M. Stuer, Z. Zhao, U. Aschauer, and P. Bowen: *J. Eur. Ceram. Soc.*, vol. 30, pp. 1335–43.
78. S. Guo, T. Nishimura, Y. Kagawa, and J. Yang: *J. Am. Ceram. Soc.*, 2008, vol. 91, pp. 2848–55.
79. R. Licheri, R. Orrù, C. Musa, A.M. Locci, and G. Cao: *J. Mater. Sci.*, 2008, vol. 43, pp. 6406–13.
80. J. Groza and A. Zavalianos: *Mater. Sci. Eng. A*, 2000, vol. A287, pp. 171–77.
81. J. Groza, M. Garcia, and J.A. Schneider: *J. Mater. Res.*, 2001, vol. 16, pp. 286–92.
82. S. Guo, Y. Kagawa, T. Nishimura, and H. Tanaka: *Ceram. Int.*, 2008, vol. 34, pp. 1811–17.